Original papers
Manufacturing processes and systems

УДК 620.178.152.34 DOI: 10.17277/jamt-2026-11-01-029-042

Peculiarities of changes in the adhesive strength of internal epoxy coatings of oil pipelines and pump-compressor pipes in hydrogen sulfide-containing environments

© Pavel E. Yudin [a,b], Maxim V. Bogatov [a,b], Aleksandr S. Lozhkomoev [c]✉

[a] *Research and Production Center "Samara" LLC, 3 B, Garazhny proezd St., Samara, 443022, Russian Federation,*
[b] *Samara State Technical University, 244, Molodogvardeyskaya St., Samara, 443100, Russian Federation,*
[c] *Panin Institute of Strength Physics and Materials Science of SB RAS, 2/4, Akademichesky Av., Tomsk, 634055, Russian Federation*

✉ asl@ispms.ru

Abstract. The paper examines the impact of hydrogen sulfide (H_2S) on the adhesion strength of internal polymer coatings designed to safeguard oil pipelines against corrosion. The analysis focuses on the mechanisms of coating destruction in aggressive environments, including the chemical reaction of H_2S with inorganic fillers such as iron oxide (Fe_2O_3), which leads to the formation of sulfides and a sharp decrease in adhesion. Experiments were conducted under autoclave conditions with varying H_2S concentrations, temperatures, and holding times. The results showed that even minimal H_2S concentrations significantly deteriorate the adhesive properties of coatings. A model of adhesion reduction is proposed that allows to predict the service life of coatings under specific operating conditions. Particular attention is given to comparing various types of coatings, including duplex, liquid, and powder systems, as well as the role of phenolic primers in their stability. The processes of diffusion and chemical interaction with the coating components were found to play a key role in durability. These findings are crucial for developing more effective anti-corrosion solutions in the oil and gas industry.

Keywords: epoxy coatings; autoclave complex; coating resource; long-term exposure; adhesive strength; corrosion processes; diffusion processes; prediction of a decrease in adhesive strength.

For citation: Yudin PE, Bogatov MV, Lozhkomoev AS. Peculiarities of changes in the adhesive strength of internal epoxy coatings of oil pipelines and pump-compressor pipes in hydrogen sulfide-containing environments. *Journal of Advanced Materials and Technologies*. 2026;11(1):029-042. DOI: 10.17277/jamt-2026-11-01-029-042

Особенности изменения адгезионной прочности внутренних эпоксидных покрытий нефтепроводных и насосно-компрессорных труб в сероводородсодержащих средах

© П. Е. Юдин [a,b], М. В. Богатов [a,b], А. С. Ложкомоев [c]✉

[a] *ООО «Научно-производственный центр «Самара», ул. Гаражный проезд, 3 Б, Самара, 443022, Российская Федерация,*
[b] *Самарский государственный технический университет, ул. Молодогвардейская, 244, Самара, 443100, Российская Федерация,*
[c] *Институт физики прочности и материаловедения им. В. Е. Панина СО РАН, пр. Академический, 2/4, Томск, 634055, Российская Федерация*

✉ asl@ispms.ru

Аннотация. Исследуется влияние сероводорода (H_2S) на адгезионную прочность внутренних полимерных покрытий, используемых для защиты нефтяных трубопроводов от коррозии. Основное внимание уделено анализу механизмов разрушения покрытий в агрессивных средах, включая химические реакции H_2S с неорганическими наполнителями, такими как оксид железа (Fe_2O_3), что приводит к образованию сульфидов и резкому снижению

адгезии. Эксперименты проводились в автоклавных условиях с варьированием концентрации H_2S, температуры и времени выдержки. Результаты показали, что даже минимальные концентрации H_2S (> 300 Па) вызывают значительное ухудшение адгезионных свойств покрытий. Предложена модель снижения адгезии, которая позволяет прогнозировать ресурс покрытий в конкретных условиях эксплуатации. Особое внимание уделено сравнению различных типов покрытий, включая дуплексные, жидкие и порошковые системы, а также роли фенольных праймеров в их устойчивости. Установлено, что процессы диффузии и химического взаимодействия с компонентами покрытий играют ключевую роль в их долговечности. Полученные данные важны для разработки более эффективных антикоррозионных решений в нефтегазовой отрасли.

Ключевые слова: эпоксидные покрытия; автоклавный комплекс; ресурс покрытия; длительная выдержка; адгезионная прочность; коррозионные процессы; диффузионные процессы; прогноз снижения адгезионной прочности.

Для цитирования: Yudin PE, Bogatov MV, Lozhkomoev AS. Peculiarities of changes in the adhesive strength of internal epoxy coatings of oil pipelines and pump-compressor pipes in hydrogen sulfide-containing environments. *Journal of Advanced Materials and Technologies*. 2026;11(1):029-042. DOI: 10.17277/jamt-2026-11-01-029-042

1. Introduction

Solving the problem of internal corrosion in oil pipelines is essential to maintaining the industry's integrity and safety. In this regard, there is active development in creating protective coatings for pipelines, including those with various polymer compositions [1–3]. Typically, the protective properties of polymer coatings are examined in NaCl solutions. However, in the oil and gas sector, corrosion is primarily caused by H_2S and CO_2 dissolved in water reacting with metal [4]. This type of corrosion is generally classified into two main categories: "sweet" and "sour" corrosion. "Sweet" corrosion occurs in environments with elevated partial pressures of H_2S and CO_2 (PH_2S and PCO_2), while "sour" corrosion occurs in environments with a PCO_2/PH_2S ratio below 20:1. These environments are further divided into three categories depending on the PCO_2/PH_2S ratio: "sweet" corrosion ($PCO_2/PH_2S > 500$), "sweet"-"sour" corrosion (PCO_2/PH_2S in the range from 20 to 500), and "sour" corrosion ($PCO_2/PH_2S < 20:1$) [5].

PH_2S and PCO_2 levels, temperature, and pH are critical factors affecting corrosion. These variables significantly influence gas dissolution, thereby affecting the rate and mechanism of corrosion product formation in sweet and sour environments. Temperature accelerates chemical reactions, but it also reduces gas solubility, which affects corrosion rates. pH levels determine the environment's acidity or alkalinity. Low pH accelerates corrosion, while high pH can trigger localized corrosion mechanisms. Dissolved CO_2 and H_2S gases form corrosive acids in water that react with metal surfaces to form less porous corrosion products, thereby accelerating corrosion. "Sweet" corrosion typically involves the formation of metal carbonates ($MeCO_3$) [6], while "sour" corrosion involves various metal sulfide formations [7].

In this regard, it is advisable to evaluate the barrier properties of polymer coatings for oil pipelines in environments containing hydrogen sulfide (H_2S) and/or carbon dioxide (CO_2). Currently, few studies in the literature address the impact of H_2S and/or CO_2 on metals protected by polymer coatings [8–13]. Even fewer publications study the mechanisms by which polymer coatings are destroyed or how aggressive components penetrate them and cause metal corrosion. The authors investigated the anticorrosion protection of a bipolar coating based on epoxy resin filled with SiO_2 particles modified with hexadecyltrimethylammonium bromide (SiO_2-CTAB) and sodium dodecylbenzenesulfonate (SiO_2-SDBS). Depending on the application sequence, when the inner layer is a *p*-type semiconductor containing SiO_2-CTAB particles and the outer layer is an *n*-type semiconductor containing SiO_2-SDBS particles (CS) or vice versa (SC), the protective action of the bipolar coating with a double electric layer changes [8].

A *p*-*n* junction is a region of space charge formed at the interface between *n*-type and *p*-type semiconductors. It exhibits high resistance. In the case of an SC coating, the inner coating adjacent to the metal substrate had fixed negative charges, such as sulfonate ions $[–SO_3]^-$, as well as mobile cations similar to those of a *p*-type semiconductor. The outer coating, which is adjacent to the solution, has fixed positive charges, such as ammonium ions $[–N(CH_3)_3]^+$, as well as mobile anions that are similar to those of an *n*-type semiconductor. When the sample was immersed in the solution, the mobile ions in the coating began to diffuse due to the

concentration gradient. This led to the formation of a *p-n* junction at the phase boundary between the inner and outer layers of the coating. When a corrosive environment, such as water and oxygen, penetrates the metal/coating phase boundary, the metal under the coating begins to oxidize. Due to the coating's cation selectivity near the metal, Fe^{2+} ions diffuse to the inner coating. However, the electric field's direction in the space charge region opposes the direction of Fe^{2+} diffusion, limiting Fe^{2+} diffusion and metal corrosion. Corrosive anions, such as HS^- and S^{2-}, diffuse into the coating and into the space charge region. Thus, for SC coatings, corrosion occurs initially before a *p-n* junction forms to prevent charge transfer.

In a CS coating, the layer near the metal is positively charged and contains mobile anions, while the layer near the solution is negatively charged and contains mobile cations. When the sample is immersed in a solution, a *p-n* junction space charge region forms. An electric field is generated from the *n*-type to the *p*-type. Thus, the outer coating prevents anions, such as HS^- and S^{2-}, from penetrating the solution, and the inner layer prevents Fe^{2+} from diffusing into the coating [5].

In [9], the authors studied the protective effect of a superhydrophobic, anti-corrosive coating on a Q235 carbon steel substrate in an environment containing 3.5 % NaCl and hydrogen sulfide. The coating consisted of an upper layer of hexadecyltrimethoxysilane (HDTMS)@SiO_2 and a lower layer of epoxy resin. They demonstrated that the coating's surface creates a cushion that traps air, provides hydrophobization, and reduces contact with the corrosive environment. This prevents the formation of a local acidic state and corrosion of the metal beneath the coating.

Depending on the polymer coating's composition, its permeability to H_2S can vary greatly. Work [14] points to the abnormally low H_2S permeability in fluoropolymers, which is primarily caused by their low H_2S solubility. The authors suggest that the extremely low solubility of H_2S in fluoropolymers, in addition to low permeability, will not cause plasticization of polymer coatings. The diffusion of H_2S into polymers can also be slowed by creating barrier layers containing ZnO or Fe_2O_3, which react with H_2S, or by filling polymers with ZnO particles.

This study aims to determine how hydrogen sulfide-containing environments affect the adhesive strength of internal epoxy coatings on oil pipelines and pump-compressor pipes.

2. Materials and Methods

2.1. Materials

Various types of polymer coatings on steel plates measuring 100×50×*t* mm (*t* is sample thickness) were used as research objects:

1) A duplex coating consisting of a layer of iron-zinc intermetallic compound (obtained by thermodiffusion zinc coating) at the boundary with a metal plate with a thickness of ~80 μm, and a second layer in the form of a thermosetting polymer coating based on epoxy-novolac resins with a thickness of ~ 160 μm [17] (Fig. 1).

The microstructure and elemental composition of the polymer coatings were studied by scanning electron microscopy using a TESCAN VEGA3 SBH microscope with an X-act energy dispersive analysis attachment.

2) A thermosetting polymer coating based on epoxy-novolac resins with a thickness of ~ 160 μm (Fig. 2).

3) Powder coatings: Coating 1 and Coating 2 (basic powder coatings used to protect the inner surface of oil pipeline and pump-compressor pipes), applied over a phenolic or epoxy-phenolic primer layer (Primer 1 and Primer 2, respectively) (Table 1, Fig. 3). These coating systems were selected due to their widespread use in protecting pipe interiors. Primer 2 and Coating 1 are standard versions, while Primer 1 and Coating 2 are heat-resistant and can withstand maximum operating and test temperatures of up to 130 °C.

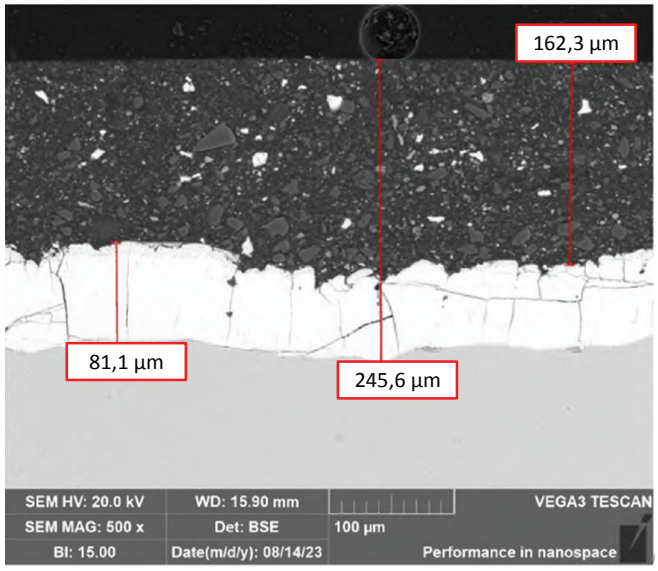

Fig. 1. Microstructure of the cross-section of the duplex coating on a metal plate

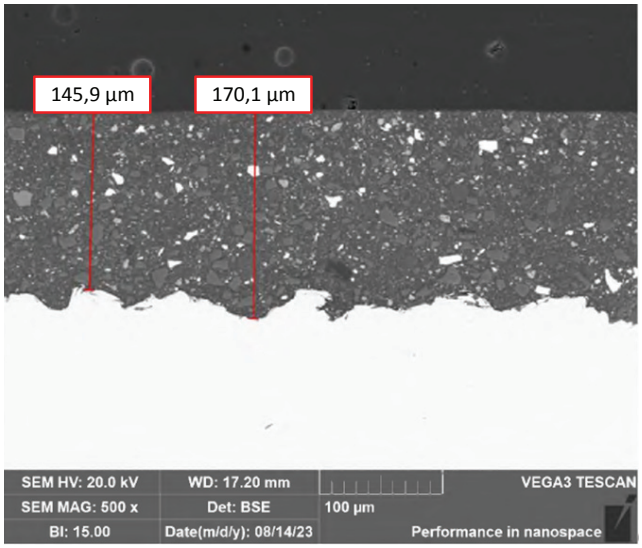

Fig. 2. Microstructure of a cross-section of a polymer coating based on epoxy-novolac resins on a metal plate

Table 1. Coating systems used as experimental samples

Number of the system tested	1	2	3
Marking in the experiment	Coating 1 / Primer 1	Coating 2 / Primer 1	Coating 1 / Primer 2
Primer	Phenolic	Phenolic	Epoxy-phenolic
Primer thickness, µm	7–32	8–22	13–31
Powder coating layer thickness, µm	350–800	350–800	350–800
Glass transition temperature Tg, °C	110 ± 3	160 ± 6	110 ± 3

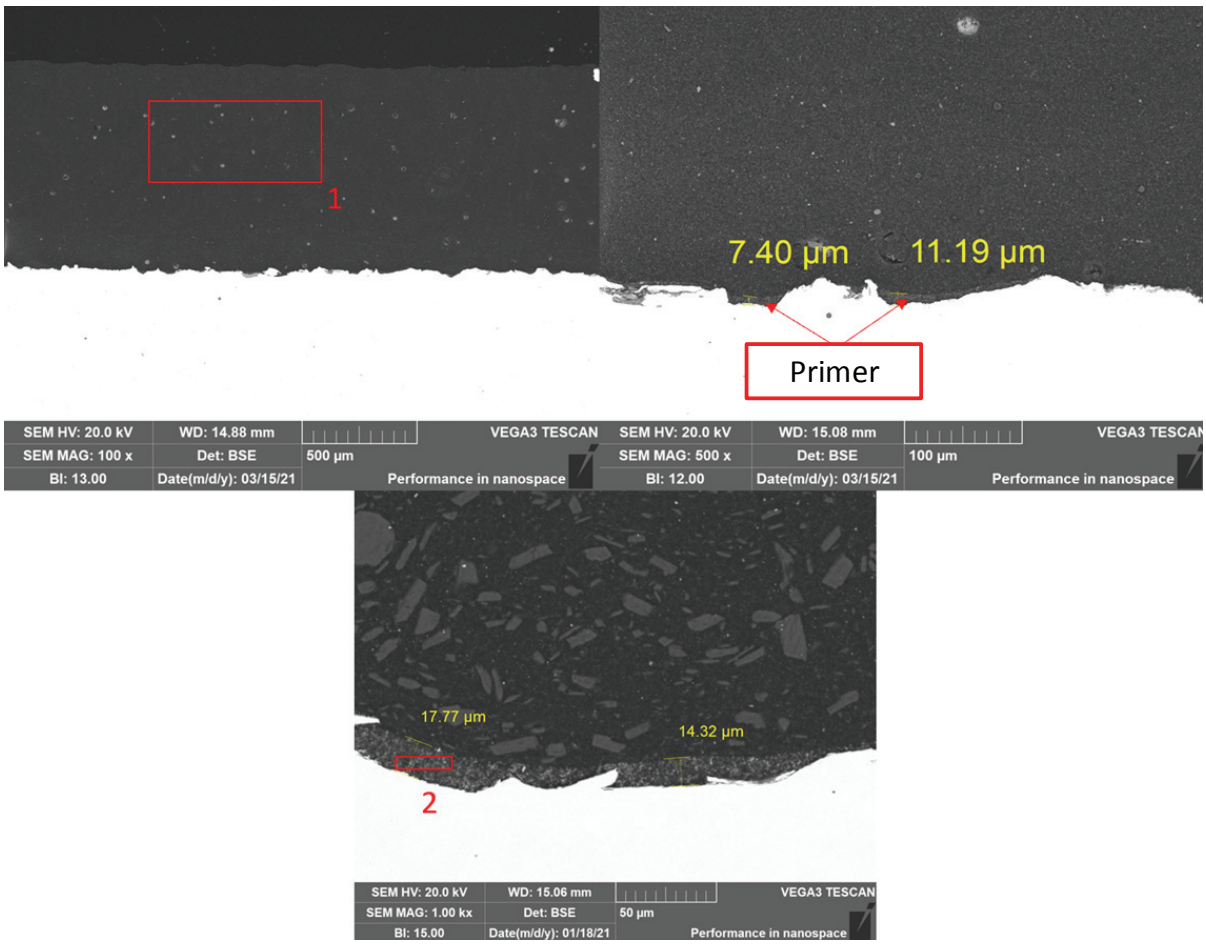

	Mass content, %								
No	C	O	Ti	Si	Al	Fe	Zn	Cr	P
1	62.88	28.06	8.29	0.42	0.35	–	–	–	–
2	47.77	25.67	0.11	1.24	0.10	21.55	2.48	0.62	0.26

Fig. 3. Microstructure of the cross-section of the Coating 1 / Primer 2 coating at different magnifications: 1 and 2 – areas of elemental analysis (* the values of inorganic inclusions may be underestimated due to the small thickness of the layer and the capture of adjacent areas of the polymer coating during analysis)

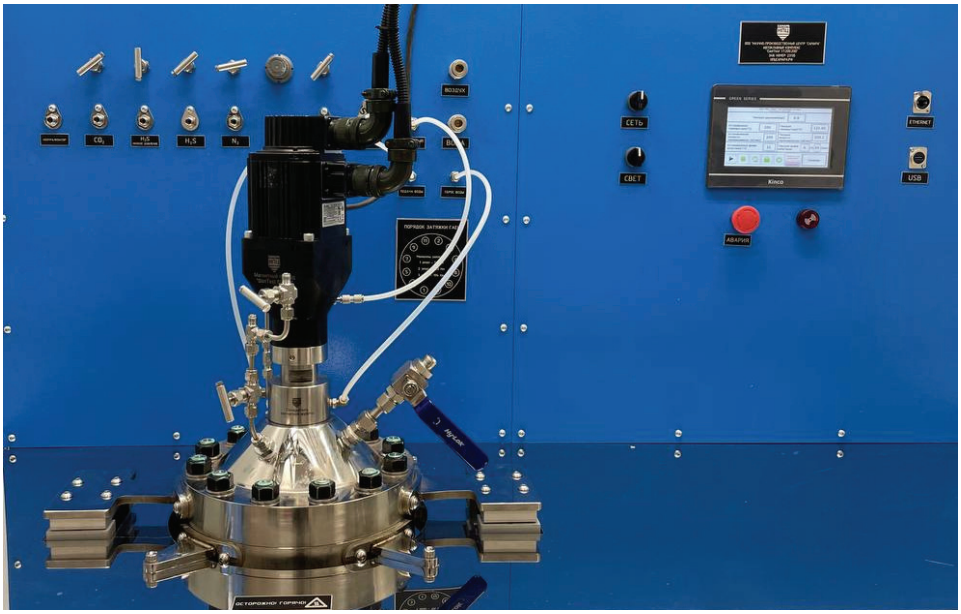

Fig. 4. Autoclave complex designed to simulate the operating conditions of tubular products during the extraction of petroleum fluid

2.2. Methodology for testing adhesive strength

In a laboratory setting, an autoclave complex (Fig. 4) was used to test the adhesive strength of the duplex coating. The tests were conducted depending on the concentration of H_2S and the adhesive strength of the coatings after exposure to various time periods in environments containing or lacking H_2S [18]. The test samples were placed in the autoclave complex. Nitrogen was blown through for five minutes to remove adsorbed oxygen from the surface of the samples and from the electrolyte solution. Then, the nitrogen pressure was reduced to atmospheric pressure. H_2S was fed into the autoclave at a temperature of (20 ± 5) °C and at the set pressure. The test medium was maintained until equilibrium was reached while keeping the H_2S pressure constant in the system. The samples were heated to the required temperature. After reaching operating mode, nitrogen was added to the total pressure. After the specified holding time, the heating was turned off, and the pressure was released. Then, the samples were removed from the autoclave and dried at 40 °C for 24 hours. After drying, the adhesion strength of the coatings was tested according to Russian Standard 32299-2013.

Three plates were tested in each experiment. The test result was taken as the arithmetic mean of six indicators obtained after the samples had been kept in the autoclave complex for the same time, following an identical period of exposure to the test environment.

The conditions for exposing the samples to the H_2S-containing environment were as follows:

– pressure of corrosive H_2S gas in the autoclave (1 ± 0.1) MPa H_2S;

– total pressure in the system (N_2) (10 ± 0.5) MPa;

– temperature (80 ± 3) °C;

– sample exposure time: 10; 20; 30; 40; 50; 60; 70; 80; 90; 100 days;

– a solution of sodium chloride in distilled water with a mass fraction of 5 % was used as the electrolyte, with an electrolyte volume of (4 ± 0.1) L.

3. Results and Discussion

The dependence of the changes in adhesive strength over time in an H_2S environment was identical for a polymer coating based on epoxy-novolac resins (liquid coating – LC) and a duplex coating (thermodiffusion zinc coating TDZ + LC) (Fig. 5).

During the first stage (the first 10 days), there is a sharp drop of more than 50% in coating adhesion in an H_2S environment. This may be due to the interaction between hydrogen sulfide and the inorganic components of the coating. The kinetics of the chemical reaction will be discussed below. This section of the experimental curve can be described by a reverse exponential function with high R^2 correlation coefficients (0.91 and 0.98). A change in color is observed in the coating, from pink (due to the red hues of Fe_2O_3 in its composition) to black (characteristic of FeS).

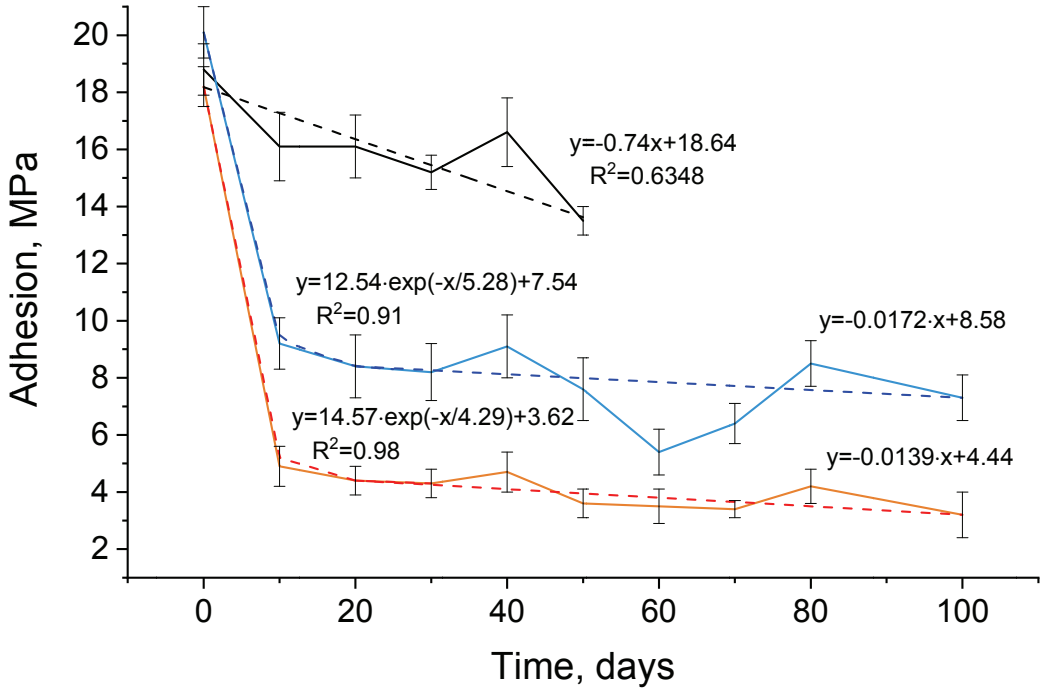

Fig. 5. Dependence of the adhesive strength of epoxy-novolac coatings on the holding time in an H_2S environment (For comparison, the dependence of the adhesive strength of a duplex coating on the holding time in an environment without H_2S is shown (black curve))

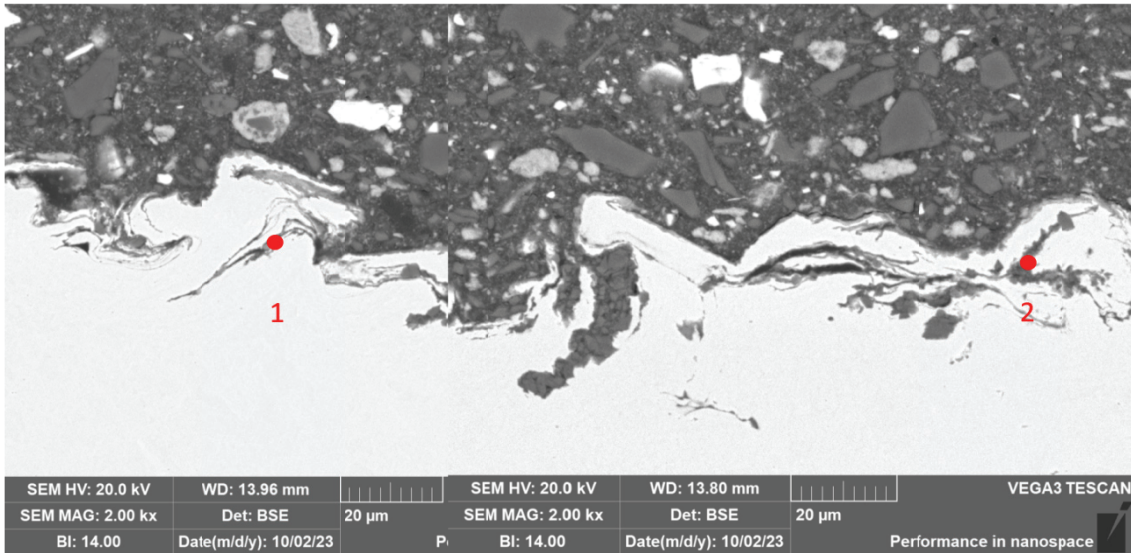

Mass content, %					
No.	C	O	S	Al	Fe
1	7.42	13.20	10.71	8.66	60.01
2	7.45	3.61	5.16	–	83.78

Fig. 6. Corrosion products represented by iron sulfides at the metal-coating interface after 100 days of exposure in a hydrogen sulfide-containing environment

This indicates that reactions are occurring within the polymer matrix. In the second stage, adhesion decreases linearly and at a slower rate. This may be due to electrolyte diffusion saturated with hydrogen sulfide and reactions at the metal-coating interface. The presence of corrosion products in the form of FeS confirms prolonged exposure (more than 70 days) (Fig. 6). The presence of an iron-zinc intermetallic sublayer does not alter the trend of decreased adhesive strength during this experiment.

This confirms the hypothesis that the dominant processes of adhesive strength reduction occur within the polymer matrix rather than at the metal-polymer interface.

During similar autoclave tests of the TDZ + LC sample in a hydrogen sulfide-free environment (Fig. 5, black curve), a gradual, linear decrease in adhesion occurred. This indicates that hydrogen sulfide decisively influences the initial decrease in coating adhesion during tests in an H_2S-containing environment.

Microstructural and elemental analyses of TDZ + LC coatings revealed that the initial sulfur distribution corresponds to the distribution of $BaSO_4$ particles in the polymer coating. These particles serve as fillers in paint and varnish materials (PVM). In areas with elevated iron content, the sulfur concentration remains at background levels (Fig. 7).

After 70 days of exposure in an H_2S-containing environment, the maximum sulfur concentration is observed in areas with localized iron (Fig. 8), indicating the occurrence of chemical reactions that lead to the formation of FeS.

SEM EDS analysis corroborates the results of local energy-dispersive analysis (Figs. 9 and 10), indicating nearly complete conversion of Fe_2O_3 to FeS. Notably, there are no morphological signs of chemical transformation: no change in the density (volume) of the filler is observed (Fig. 11*a*), and there are no cracks at its boundary (Fig. 11*b*). This may be due to the small (7.5 %) difference in density between Fe_2O_3 and FeS, as well as the polymer's good relaxation capacity, which compensates for stresses in the material and prevents cracks at the filler-polymer matrix interface. However, the formation of FeS contributes to the disruption of the primary adhesive bonds. The residual adhesive strength of the polymer coating is provided by zones free of FeS and subsequently varies according to a linear law.

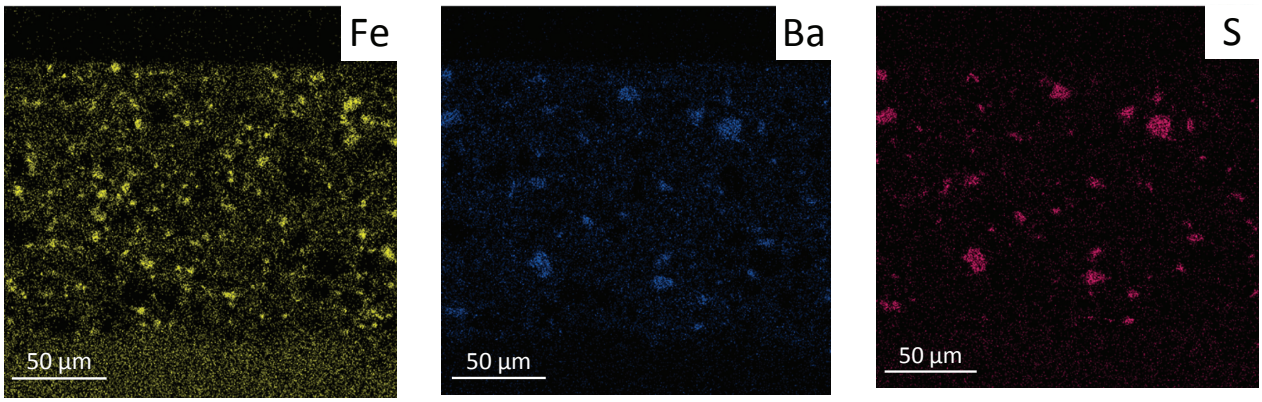

(a) *(b)* *(c)*

Fig. 7. Results of the mapping mode elemental SEMEDS analysis of the TDZ + LC section in the initial state in the characteristic radiation: *a* – Fe; *b* – Ba; *c* – S

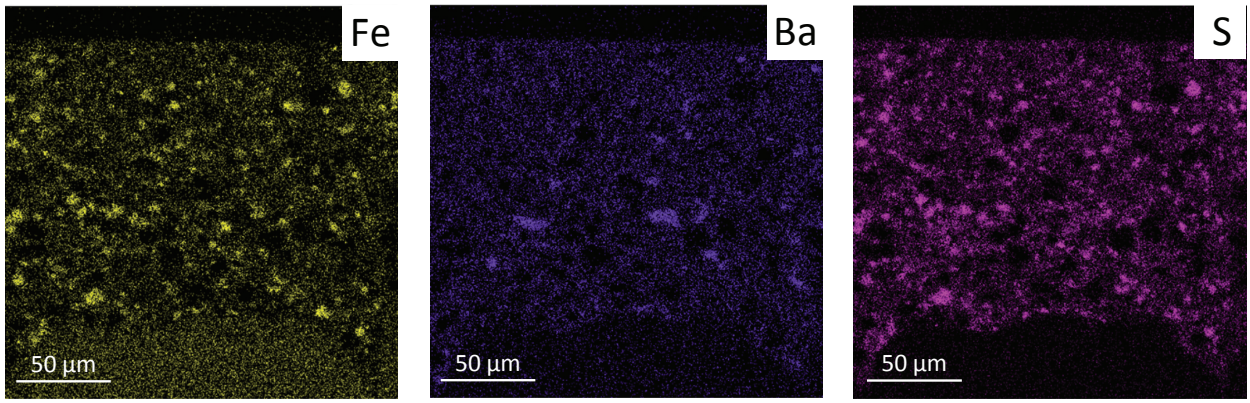

(a) *(b)* *(c)*

Fig. 8. Results of the mapping mode elemental SEMEDS analysis of the TDZ + LC section after 70 days of exposure in an H_2S environment in characteristic radiation: *a* – Fe; *b* – Ba; *c* – S

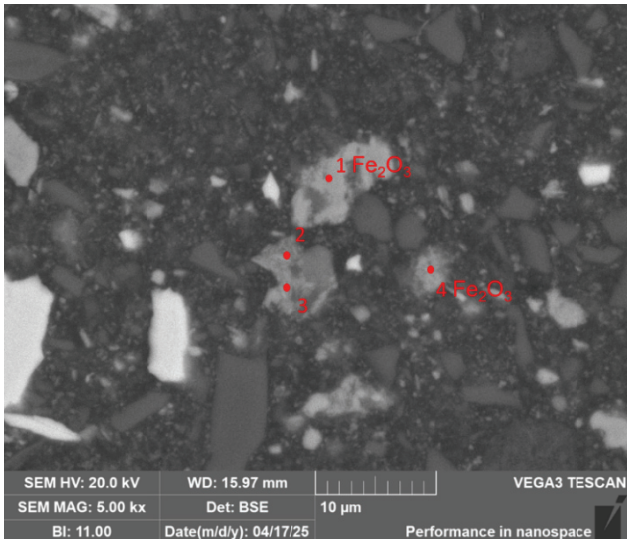

No.	Mass content, %									
	O	Fe	Si	C	Mg	Al	Ti	Ca	K	S
1	21.80	71.19	1.17	5.83	–	–	–	–	–	–
2	28.62	40.68	7.82	12.41	2.76	3.33	2.94	0.76	0.69	–
3	23.17	56.03	4.22	10.69	0.74	2.40	1.58	0.62	0.56	–
4	21.06	60.89	14.29	1.98	–	0.80	0.99	–	–	–

Fig. 9. Results of the energy dispersive analysis of inorganic fillers of the TDZ + LC system's polymer coating in the initial state

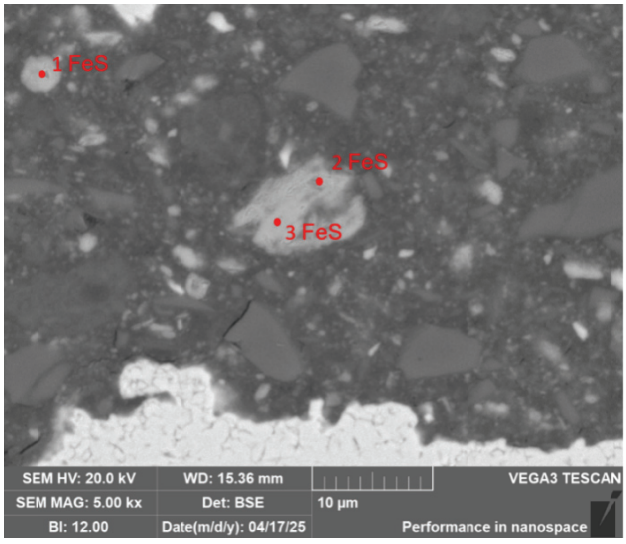

No.	Mass content, %						
	Si	S	Fe	C	O	Al	Ti
1	2.50	27.02	41.92	18.56	7.45	1.29	1.27
2	0.85	32.11	43.92	13.62	8.17	0.64	0.69
3	0.45	34.30	54.62	6.74	3.52	0.38	–

Fig. 10. Results of the energy dispersive analysis of inorganic fillers of the TDZ + LC system's polymer coating after exposure to a hydrogen sulfide-containing environment for 70 days

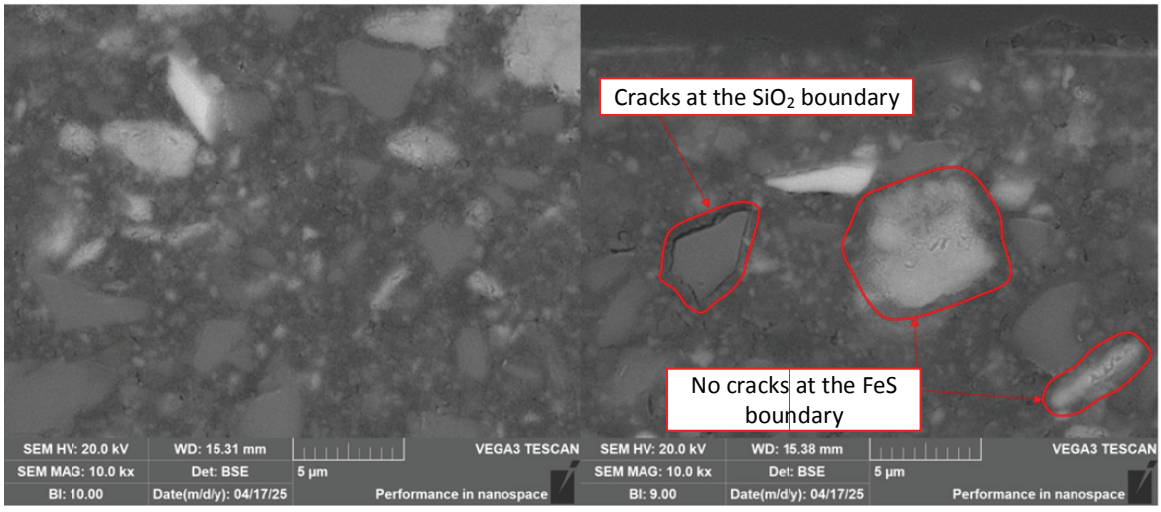

(a) *(b)*

Fig. 11. Microstructural studies of TDZ + LC:
a – in the initial state; *b* – after exposure to a hydrogen sulfide-containing environment for 70 days

After 70 days of exposure to H_2S, isolated cracks are detected at the boundaries of SiO_2 particles in the polymer coating. These cracks do not significantly affect the reduction in coating adhesion (Fig. 11).

Thus, the sharp decrease in epoxy-novolac coating adhesion during the first ten days of testing is directly linked to chemical reactions between hydrogen sulfide and the coating's fillers (primarily Fe_2O_3). In this regard, the dependences of adhesion on test duration in an H_2S environment obtained (Fig. 5) can be correlated with the kinetics of the coating's chemical reactions. Initially, adhesion changes are determined by the rate at which H_2S is supplied to the coating, diffuses to the Fe_2O_3 particles, and undergoes direct chemical transformation. In this case, the formation of a surface layer of iron sulfide on the particle surfaces,

which likely occurs within the first 10 days, is sufficient to maximize the reduction in adhesion. Meanwhile, the reaction of the filler particles with hydrogen sulfide continues. Assuming that the adhesion value (σ) is a function of H_2S consumption when interacting with coating components (Q), the data in Fig. 5 can be used to plot Q as a function of autoclave test time (t), with Q equal to $\sigma(t_0) - \sigma(t)$. In this case, $\sigma(t_0)$ is the initial adhesion and $\sigma(t)$ is the adhesion at time t (see Fig. 12).

In the case of a pseudo-first-order reaction, the initial segments of the obtained curves can be expressed in differential form as follows (1):

$$\frac{dQ_t}{dt} = k_1(Q_{\max} - Q_t), \qquad (1)$$

where k_1 is the first-order rate constant, min^{-1}; $Q_{\max}$ is the maximum H_2S consumption; Q_t is the H_2S consumption at time t, and t is time, min.

Integrating equation (1) under the boundary conditions $Q_t = 0$ at $t = 0$ and $Q_t = Q_t$ at $t = t$ yields a linear relationship, and plotting the values of $\ln(Q_{\max}/(Q_{\max} - Q_t))$ as a function of t gives a slope that can be used to determine the first-order reaction rate constant (2):

$$\ln\left[\frac{Q_{\max}}{Q_{\max} - Q_t}\right] = k_1 t. \qquad (2)$$

A pseudo-second-order reaction can be described by equation (3):

$$\frac{dQ_t}{dt} = k_2(Q_{\max} - Q_t)^2. \qquad (3)$$

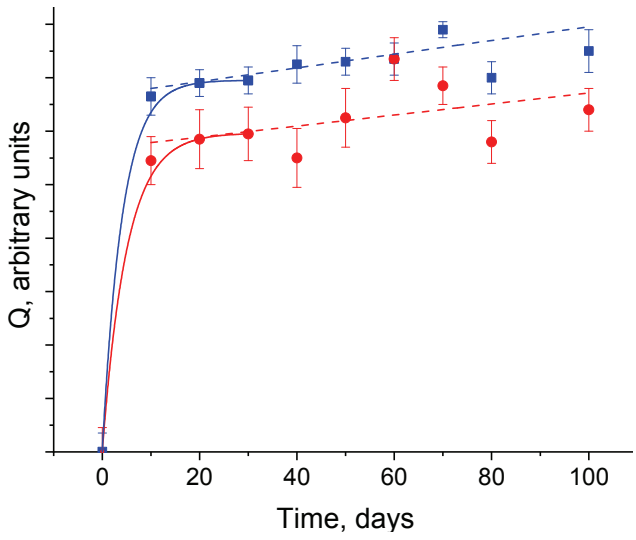

Fig. 12. Kinetic dependences of the parameter Q (duplex coating TDZ + LC – red curve; polymer coating LC – blue curve)

Integrating equation (3) using the boundary conditions $Q_t = 0$ at $t = 0$ and $Q_t = Q_t$ at $t = t$ yields:

$$\frac{1}{Q_{\max} - Q_t} - \frac{1}{Q_{\max}} = k_2 t \qquad (4)$$

or

$$Q_t = \frac{Q_{\max}^2 k_2 t}{1 + Q_{\max} k_2 t}. \qquad (5)$$

The linear form of equation (5) is as follows

$$\frac{t}{Q_t} = \frac{t}{Q_s} + \frac{1}{Q_{\max}^2 k_2} \qquad (6)$$

or

$$\frac{t}{Q_t} = \frac{t}{Q_s} + \frac{1}{m}, \qquad (7)$$

where m denotes the initial diffusion rate coefficient and is equal to $Q_{\max}^2 k_2$.

By plotting the graph $t/Q_t = f(t)$, one can determine the initial diffusion rate m, $Q_{\max}$, and the pseudo-second-order rate constant k_2.

Figure 13 shows the linearized forms of the first- and second-order Q versus t dependences. Higher R^2 values are observed for second-order kinetic models compared to first-order kinetic models. This indicates that the second-order model is more suitable for describing changes in adhesion in an H_2S environment and that the process consists of multiple mechanisms.

When obtaining the dependence at three different temperatures, the slopes of the lines in Figs. 13*c* and 13*d* will change. It is then possible to determine the activation energy and the Arrhenius constant by plotting graphs of $\ln(k_2)$ versus T.

Using the TDZ + LC coating as an example, an assessment of H_2S concentration was conducted during autoclave tests for adhesive strength after 336 hours of treatment. The system parameters during the tests were as follows:

– the H_2S concentration was varied by injecting 0.1, 0.5, 1, or 1.5 MPa of corrosive gas into the system;

– the total pressure in the system was regulated by nitrogen to (10 ± 0.5) MPa;

– temperature (90 ± 3) °C;

– the electrolyte was a 5 % sodium chloride solution in distilled water, with a volume of (4 ± 0.1) L.

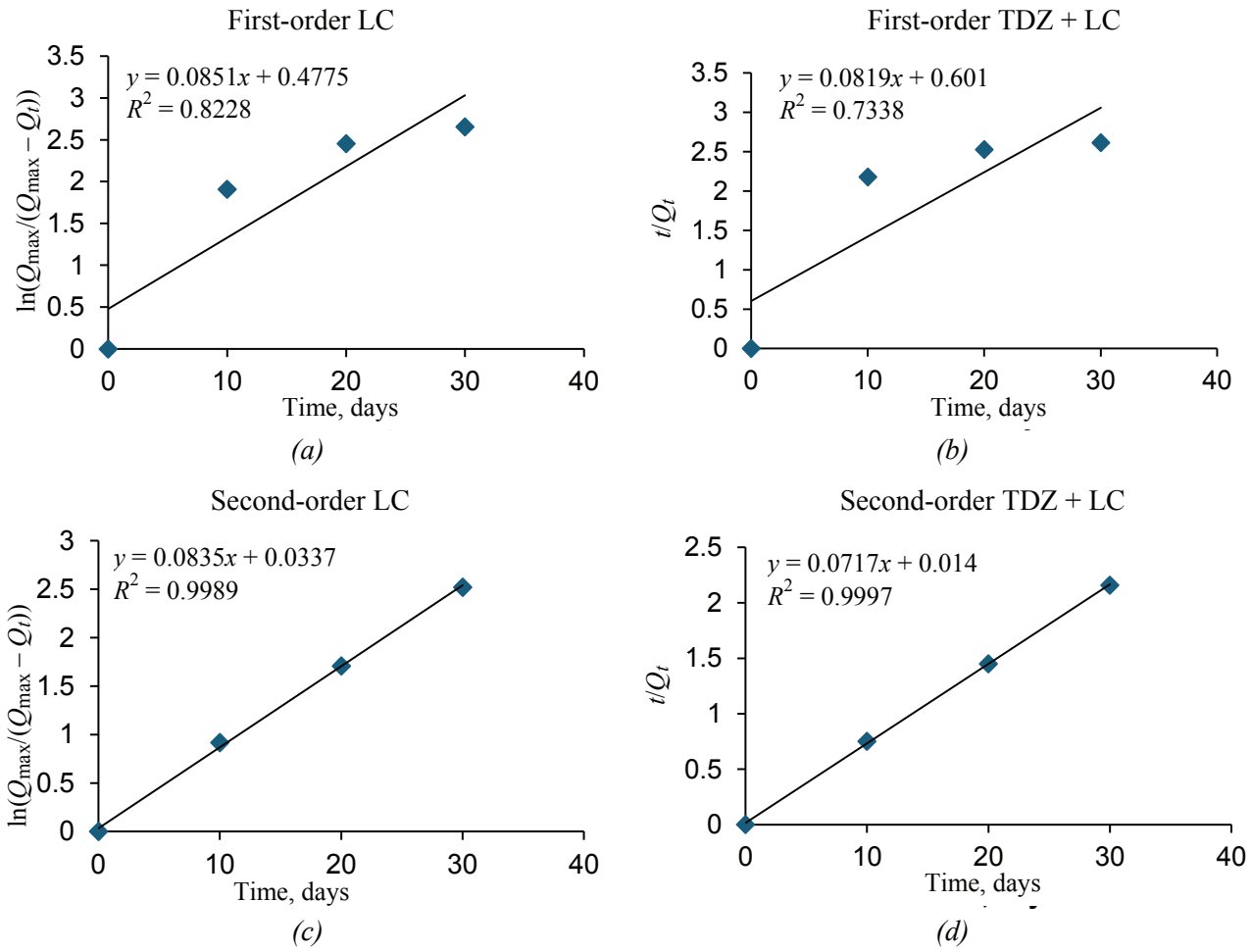

Fig. 13. Linear forms of pseudo-first-order (*a*, *b*) and pseudo-second-order (*c*, *d*) kinetic equations for the interaction of hydrogen sulfide with epoxy-novolac coatings

The test results are presented in Fig. 14. As can be seen, the adhesive strength function as a function of H_2S concentration in the system is described by an equation of the form $y = a \times x^b$, where $a = 3.255$, $b = –0.205$, with a correlation coefficient $R^2 = 0.98$. A significant decrease in adhesive strength, from 13.8 to 5.0 MPa, is achieved even at the minimum H_2S content under experimental conditions. An increase in hydrogen sulfide concentration from 0.1 to 1.5 MPa does not significantly decrease adhesion. These results indicate the need to evaluate the barrier properties of coatings intended for wells with low partial pressures of hydrogen sulfide, starting from 300 Pa. At such H_2S concentrations, wells are classified as corrosion-prone.

Figure 15 shows the dependence of the adhesive strength of powder coatings on exposure duration to a hydrogen sulfide-containing environment. The obtained data can be approximated by linear functions corresponding to the 10–100 day range for LC (Fig. 5).

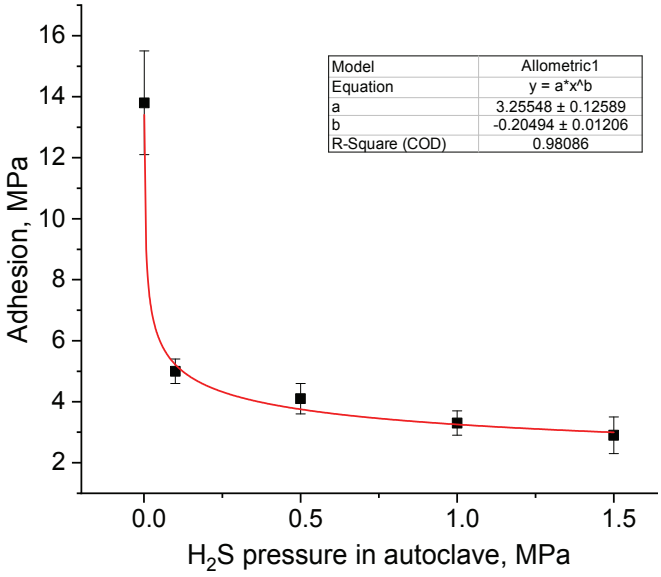

Fig. 14. Change in the adhesive strength of the TDZ + LC coating depending on the concentration of H_2S in the autoclave

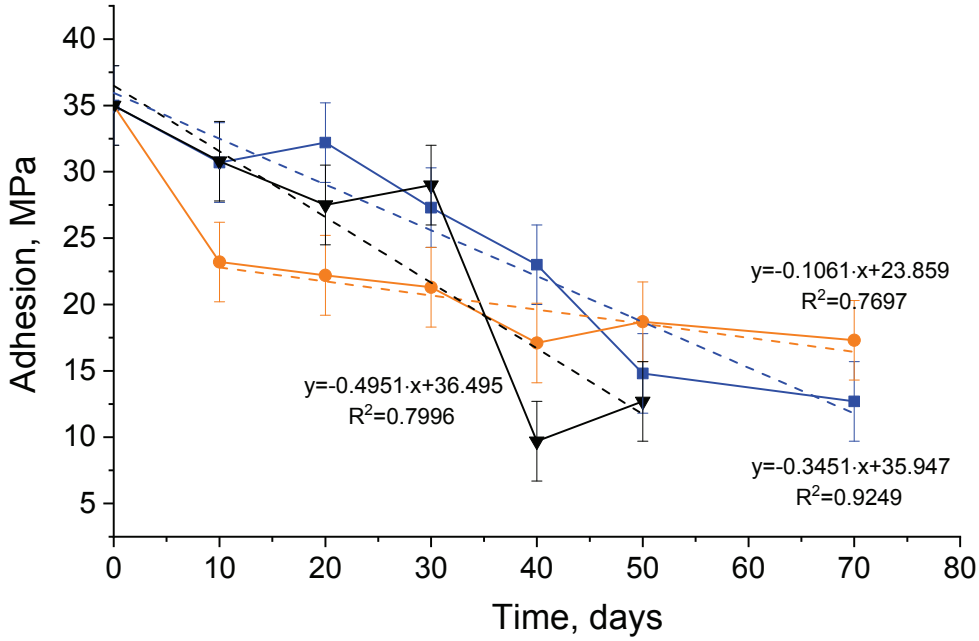

Fig. 15. Dependences of the adhesion strength of powder coatings on the treatment time in an H_2S environment (Coating 1 / Primer 1 –straight orange line, Coating 2 / Primer 1– straight blue line, Coating 1 / Primer 2 – straight black line)

Table 2. Adhesion reduction after an autoclave test of three types of coatings in hydrogen sulfide-containing environment

Coating system / Test temperature	Coating 1 / 80 °C	Coating 1 / 90 °C	Coating1 / Primer 2 / 80 °C
Adhesion value, MPa	17.0 ± 3.5	20.2 ± 2.9	9.4 ± 2.2
Adhesion reductionas compared to initial value, %	32	19	62

In this case, it can be assumed that no chemical reactions occur in the coating or at the metal-coating interface during the initial stages of treatment. Instead, there is gradual diffusion of corrosion-active components, with reactions occurring within the polymer volume and at the metal-coating interface. This is confirmed by a change in the nature of corrosion, from predominantly cohesive to fully adhesive. For the 0–10 day period, significant deviation from the straight line is observed for the Coating 1/Primer 1 system. This deviation may be due to chemical reactions occurring during this time. Of interest is the tangent of the slope of the approximating straight line. The gray line plotted for the Coating 1/Primer 2 system has the highest slope (0.495), which corresponds to the empirical data. Systems with a simple phenolic primer of the Primer 2 type have a service life that is 30–50 % shorter than similar powder coatings with Primer 1. Additionally, it is evident that using a high-temperature material does not provide any additional benefits.

Powder coatings typically use a phenolic primer containing up to 50 % iron oxide (Fe_2O_3) (Fig. 4). At a diffusion rate significantly higher than the diffusion coefficient (D), the coatings in Fig. 3 are characterized by chemical reactions between the primer and hydrogen sulfide.

One telling example is the experiment that evaluated the reduction in adhesion of a powder coating with and without a primer. The experiment involved autoclave treatment of Coating 1 with Primer 2 and without a primer at 80 and 90 °C, as described in Section 2. As shown in Table 2, the decrease in adhesion is 32 % and 19 % at 80 and 90 °C, respectively, for the system without a primer, while it is 62 % for the system with a primer at 80 °C. This significant difference in adhesion change is due to the primer's reaction with hydrogen sulfide to form iron sulfide (Fig. 16). The values for the experiment at 80 and 90 °C fall within the confidence interval. The typical composition of a primer similar to Primer 2 is presented in Table 3. As can be seen, the iron oxide content reaches 33 %, and its reaction with hydrogen sulfide leads to a significant drop in adhesion. This mechanism is similar to that described above for the liquid epoxy-novolac coating.

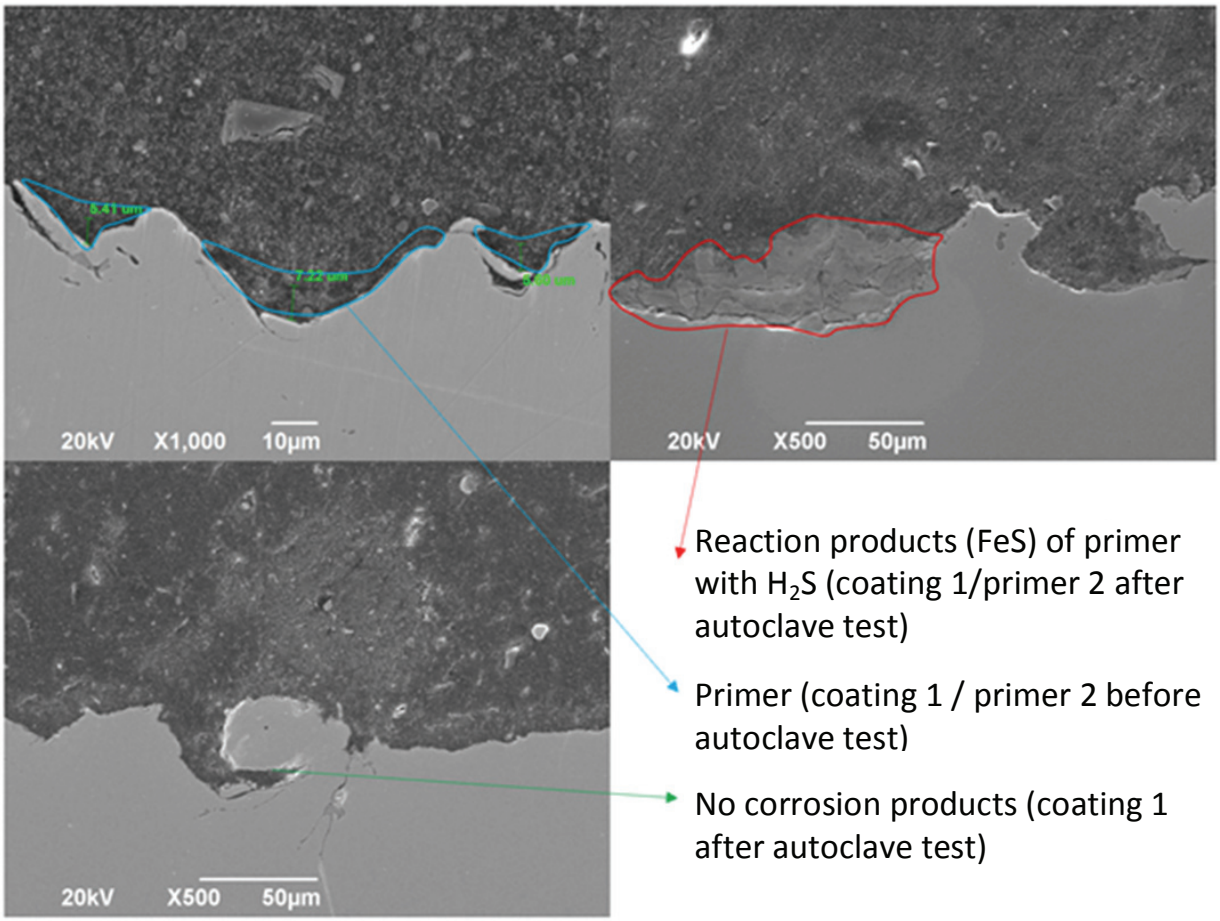

Fig. 16. State of the metal/coating interface before and after the autoclave test at a temperature of +80 °C

Table 3. Typical primer composition

Primer component	Approximate mass concentration, %
Butyl cellosolve	25
Phenolformaldehyde resin	19
Toluene	32
High-molecular-weight epoxy resin	9
Iron oxide pigment	14
Aerosil R 974	1

Substances forming the dry residue are written in italics.

In summary, the decrease in coating adhesion in environments containing hydrogen sulfide can be described by equation (8) for the general case:

$$\sigma(t) = k_1 \, e^{-t/k_2} + k_3 t + \sigma_0. \quad (8)$$

The ratio of the coefficients k_1, k_2, and k_3 depends on the amount of fillers that react with hydrogen sulfide. In their absence, the relationship becomes linear. Knowing the tangent of the angle of inclination of the segment described by the line allows one to predict the exposure time before the peeling process begins (i.e., the limit values at which the coatings retain their protective properties). Considering that coating degradation proceeds identically under laboratory and field conditions, this equation can also be used to estimate the remaining service life of pipes with anticorrosion coatings when the coefficients k_1, k_2, and k_3 are selected.

4. Conclusion

A pattern has been established for the first time for the decrease in adhesion of polymer coatings following exposure to a hydrogen sulfide-containing environment. This decrease is caused by the reaction of iron oxide, a component of the coating's inorganic fillers, and the diffusion of water containing dissolved corrosive gases toward the metal. At the beginning of exposure, the change in adhesion is determined by the rate at which H_2S is supplied to the coating, diffuses to the Fe_2O_3 filler particles, and undergoes direct chemical transformation. The dependence of the change in adhesion on the partial pressure of H_2S has been shown to be

inversely proportional. For coatings whose components react with hydrogen sulfide, even low partial pressures of H_2S (> 300 Pa) are critical, regardless of the initial values of adhesive strength. For steady-state modes of adhesive bond disruption, H_2S's contribution is insignificant; in this case, water absorption and mass transfer processes dominate.

After the chemical reactions have completed, the decrease in adhesion is linear. Given the slope of the line for specific operating or test conditions, one can predict how long it will take for the adhesive strength to drop to zero. Considering the similarity of degradation processes under laboratory and field conditions (except for process intensity), the obtained results allow to predict the remaining service life of pipeline coatings.

5. Funding

This work was partially carried out as part of a state-funded project at the Panin Institute of Strength Physics and Materials Science of the Siberian Branch of the Russian Academy of Sciences (ISPMS SB RAS), Grant No. FWRW-2026-0004.

Финансирование

Работа частично выполнена в рамках государственного задания ИФПМ СО РАН, тема FWRW-2026-0004.

6. Conflict of interests

The authors declare no conflict of interests.

Конфликт интересов

Авторы заявляют об отсутствии конфликта интересов.

References

1. Nazar R, Mehmood U, Ahmed H, Imran A, et al. Smart polymers coating for upstream oil and gas industry to slow down the corrosion. In: Jafar Mazumder M, Quraishi M, Al-Ahmed A, editors. *Polymeric Corrosion Inhibitors for Greening the Chemical and Petrochemical Industry*. 1st edn Wiley; 2022. p. 331-352. DOI:10.1002/9783527835621.ch13

2. De Leon ACC, Da Silva ÍGM, Pangilinan KD, Chen Q, et al. High performance polymers for oil and gas applications. *Reactive and Functional Polymers*. 2021;162: 104878. DOI:10.1016/j.reactfunctpolym.2021.104878

3. Al Madan A, Hussein A, Akhtar SS. A review on internal corrosion of pipelines in the oil and gas industry due to hydrogen sulfide and the role of coatings as a solution. *Corrosion Reviews*. 2025;43(2):189-208. DOI:10.1515/corrrev-2024-0114

4. Vakili M, Koutník P, Kohout J. Addressing hydrogen sulfide corrosion in oil and gas industries: a sustainable perspective. *Sustainability*. 2024;16(4):1661. DOI:10.3390/su16041661

5. Shi X, Zhang Z, Wu L, Li X, et al. Corrosion law of metal pipeline in Tahe Oilfield and application of new materials. *Coatings*. 2021;11(11):1269. DOI:10.3390/coatings11111269

6. Videm K, Koren AM. Corrosion, passivity, and pitting of carbon steel in aqueous solutions of HCO_3^-, CO_2, and Cl^-. *Corrosion*. 1993;49(9):746-754. DOI:10.5006/1.3316127

7. Obot IB, Solomon MM, Umoren SA, Suleiman R, et al. Progress in the development of sour corrosion inhibitors: past, present, and future perspectives. *Journal of Industrial and Engineering Chemistry*. 2019;79:1-18. DOI:10.1016/j.jiec.2019.06.046

8. Dong Y, Zhou Q, Meng X, Cong C, et al. Anti-H_2S corrosion property of bipolar epoxy-resin coatings. *Progress in Organic Coatings*. 2019;130:66-74. DOI:10.1016/j.porgcoat.2019.01.036

9. Zeng Q, Kang L, Fan J, Song L, et al. Durable superhydrophobic silica/epoxy resin coating for the enhanced corrosion protection of steel substrates in high salt and H_2S environments. *Colloids and Surfaces A: Physicochemical and Engineering Aspects*. 2022; 654:130137. DOI:10.1016/j.colsurfa.2022.130137

10. Banan A, Asadi S. Novel cationic and non-ionic biopolyurethanes for effective inhibition of mild steel corrosion in H_2S-CO_2 environment. *Industrial Crops and Products*. 2024;221:119320. DOI:10.1016/j.indcrop.2024.119320

11. Yudin P, Petrov S, Maximuk A, Knyazeva Z. Destruction mechanisms and methods of laboratory autoclave tests of internal coatings of oil pipes. *E3S Web of Conferences*. 2019;121:01009. DOI:10.1051/e3sconf/201912101009

12. Shaikhah D, Taleb W, Mohamed-Said M, Cowe B, et al. Augmentation of polymer-$FeCO_3$ microlayers on carbon steel for enhanced corrosion protection in hydrodynamic CO_2 corrosion environments. *ACS Omega*. 2024;9(29):31745-31753. DOI:10.1021/acsomega.4c02616

13. Lauer R. Novel internal coating system for high concentration H_2S environments. In: *International Petroleum Exhibition & Conference IPTC 2022. Abu Dhabi, February 2022,* UAE: SPE; 2019. p. D021S037R001. DOI:10.2118/197950-MS

14. Merkel TC, Toy LG. Comparison of hydrogen sulfide transport properties in fluorinated and nonfluorinated polymers. *Macromolecules*. 2006; 39(22):7591-7600. DOI:10.1021/ma061072z

15. Lefebvre X, Pasquier D, Gonzalez S, Epsztein T, et al. Development of reactive barrier polymers against corrosion for the oil and gas industry: from formulation to qualification through the development of predictive multiphysics modeling. *Oil & Gas Science and Technology – Revue d'IFP Energies nouvelles*. 2015; 70(2):291-303. DOI:10.2516/ogst/2015001

16. Shi X, Zhu K, Yuan X. Improvement of mechanical properties of highly ZnO-filled polyethylene

composites by dual-compatibilizer for hydrogen sulfide permeation inhibition. *Polymers for Advanced Technologies*. 2024;35(4):e6377. DOI:10.1002/pat.6377

17. Yudin PE. Functional coatings for downhole oilfield equipment for protection against corrosion, asphalt-resin-paraffin and salt deposits: Review. *Izvestiya vysshikh uchebnykh zavedeniy. Poroshkovaya Metallurgiya i Funktsional'nye Pokrytiya = Russian Journal of Non-Ferrous Metals*. 2025;19(1):58-74. DOI:10.17073/1997-308X-2025-1-58-74 (In Russ.)

18. Aleksandrov EV, Yudin PE, Knyazeva ZhV. The new technique of autoclave test for the rapid analysis of anticorrosion coatings. *Truboprovodnyj transport: teoriya i praktika*. 2015;3(49):3-11. (In Russ.)

Information about the authors / Информация об авторах

Pavel E. Yudin, Cand. Sc. (Eng.), Associate Professor, Director of Science, Research and Production Center "Samara" LLC, Samara State Technical University, Samara, Russian Federation; ORCID 0000-0002-4517-3744; e-mail: udin@npcsamara.ru

Maxim V. Bogatov, Cand. Sc. (Eng.), Associate Professor, Leading Engineer, Research and Production Center "Samara" LLC, Samara State Technical University, Samara, Russian Federation; ORCID 0000-0002-6232-5666; e-mail: bogatov@npcsamara.ru

Aleksandr S. Lozhkomoev, D. Sc. (Eng.), Leading Researcher, Panin Institute of Strength Physics and Materials Science of SB RAS, Tomsk, Russian Federation; ORCID 0000-0002-1564-0858; e-mail: asl@ispms.ru

Юдин Павел Евгеньевич, кандидат технических наук, доцент, директор по науке, ООО «Научно-производственный центр «Самара», Самарский государственный технический университет, Самара, Российская Федерация; ORCID 0000-0002-4517-3744; e-mail: udin@npcsamara.ru

Богатов Максим Валерьевич, кандидат технических наук, доцент, ведущий инженер, ООО «Научно-производственный центр «Самара», Самарский государственный технический университет, Самара, Российская Федерация; ORCID 0000-0002-6232-5666; e-mail: bogatov@npcsamara.ru

Ложкомоев Александр Сергеевич, доктор технических наук, ведущий научный сотрудник, Институт физики прочности и материаловедения им. В. Е. Панина СО РАН, Томск, Российская Федерация; ORCID 0000-0002-1564-0858; e-mail: asl@ispms.ru

Received 16 December 2025; Revised 21 January 2026; Accepted 02 February 2026